Supplement of Atmos. Chem. Phys., 15, 11931–11948, 2015
http://www.atmos-chem-phys.net/15/11931/2015/
doi:10.5194/acp-15-11931-2015-supplement


Atmospheric Chemistry and Physics
Open Access
EGU

*Supplement of*

# Distinguishing the drivers of trends in land carbon fluxes and plant volatile emissions over the past 3 decades

**X. Yue et al.**

*Correspondence to:* X. Yue (xuyueseas@gmail.com)

**Supplement**

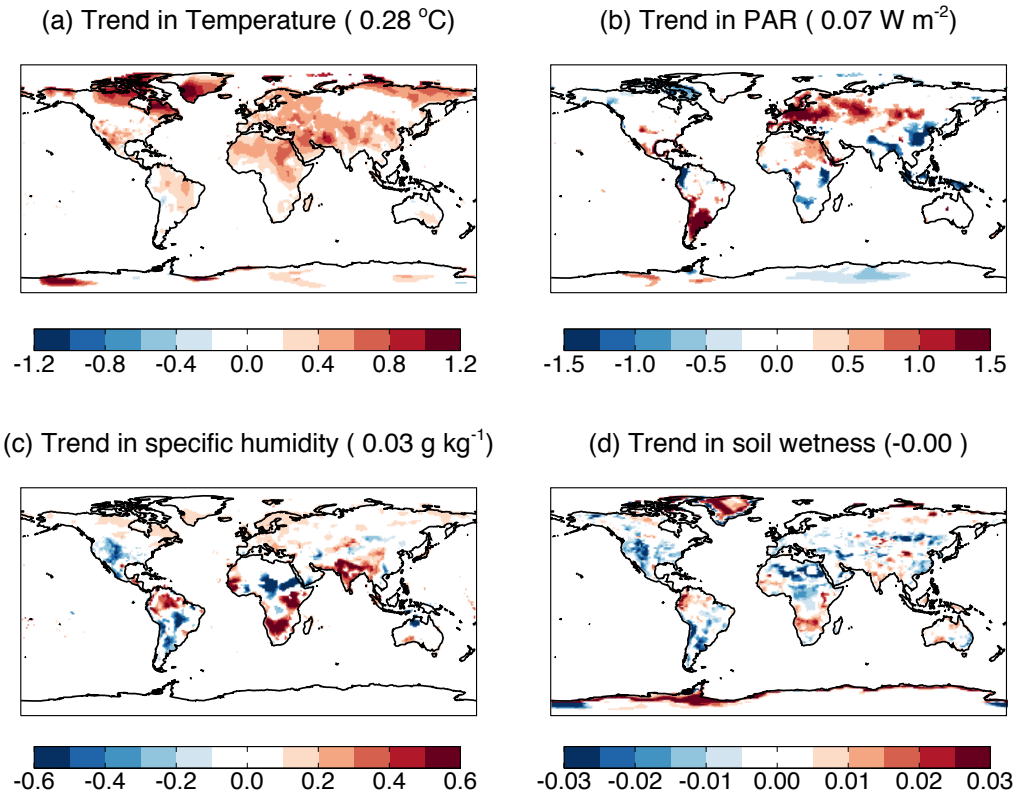


**Figure S1.** Trends in the annual mean (a) surface air temperature, (b) photosynthetically active radiation (PAR), (c) surface specific humidity, and (d) soil wetness at 1.5 m from the WFDEI reanalyses for 1982-2011. Values are shown only for trends with significance level $p < 0.05$. The global average trends are shown in the title brackets. The units of trends are (a) °C decade$^{-1}$, (b) W m$^{-2}$ decade$^{-1}$, (c) g kg$^{-1}$ decade$^{-1}$, and (d) decade$^{-1}$.

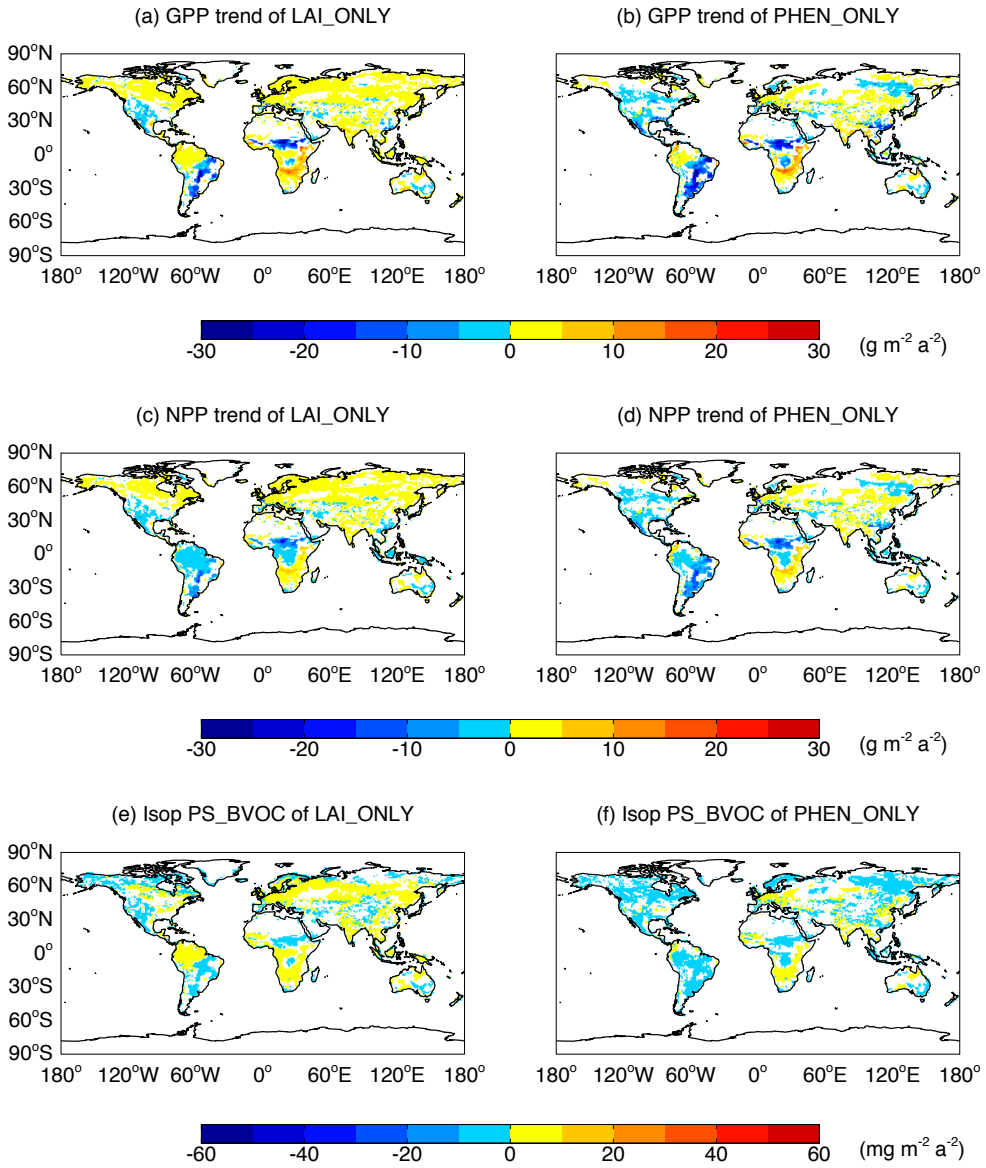


**Figure S2.** Predicted trends of (a, b) GPP, (c, d) NPP, and (e, f) Isoprene from PS_BVOC for 1982-2011 for simulations (a, c, e) LAI_ONLY and (b, d, f) PHEN_ONLY. Only significant trends ($p < 0.05$) are presented. Isoprene emissions with MEGAN scheme (not shown) exhibit very similar responses to LAI and phenological changes as that with PS_BVOC scheme.

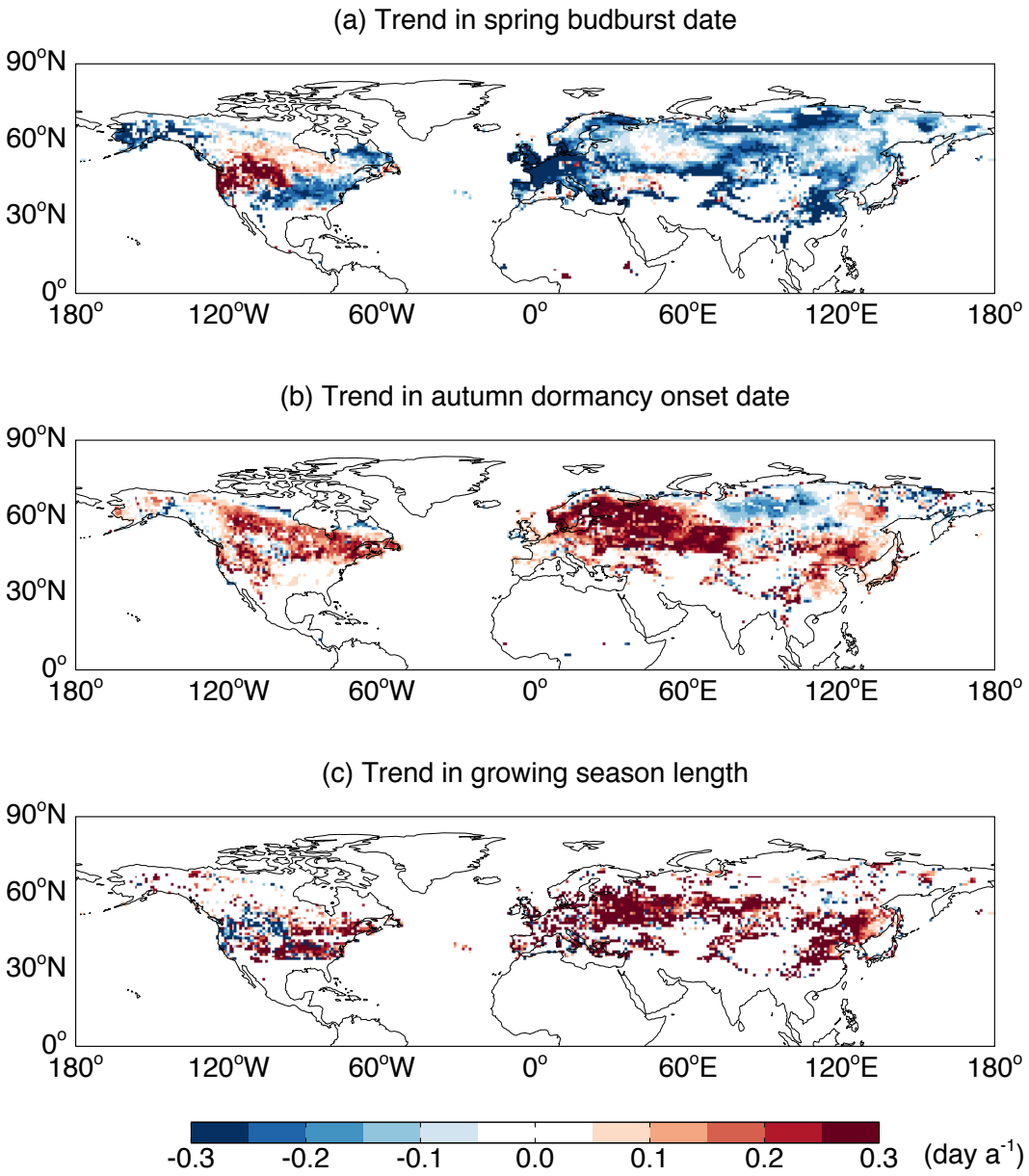


**Figure S3.** Predicted trends in (a) budburst date, (b) dormancy onset date, and (c) growing season length during 1982-2011. Simulated phenological dates in each grid square are the composite results from DBF, tundra, shrubland, and grassland based on PFT fraction and LAI in that grid box. Simulations are performed with WFDEI reanalysis.

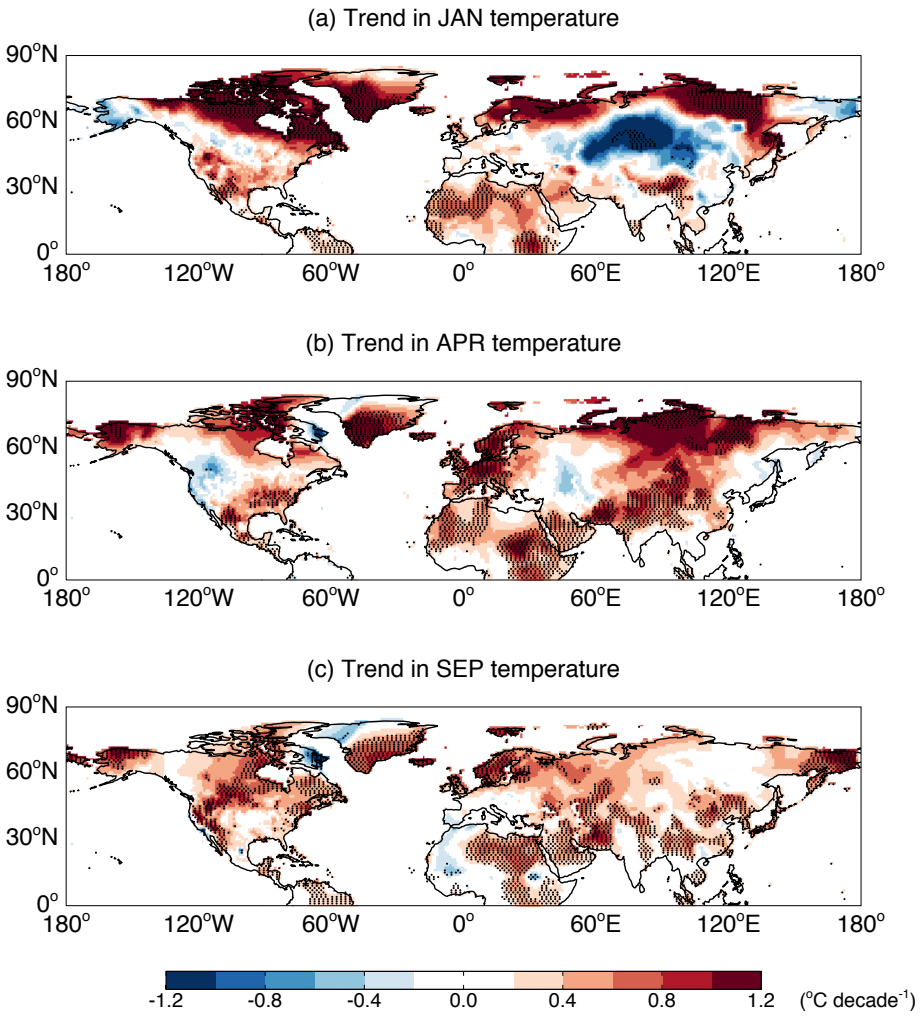


**Figure S4.** Trends in the surface air temperature of (a) January, (b) April, and (c) September from the WFDEI reanalyses for 1982-2011. Significant trends ($p < 0.05$) are denoted with dots.

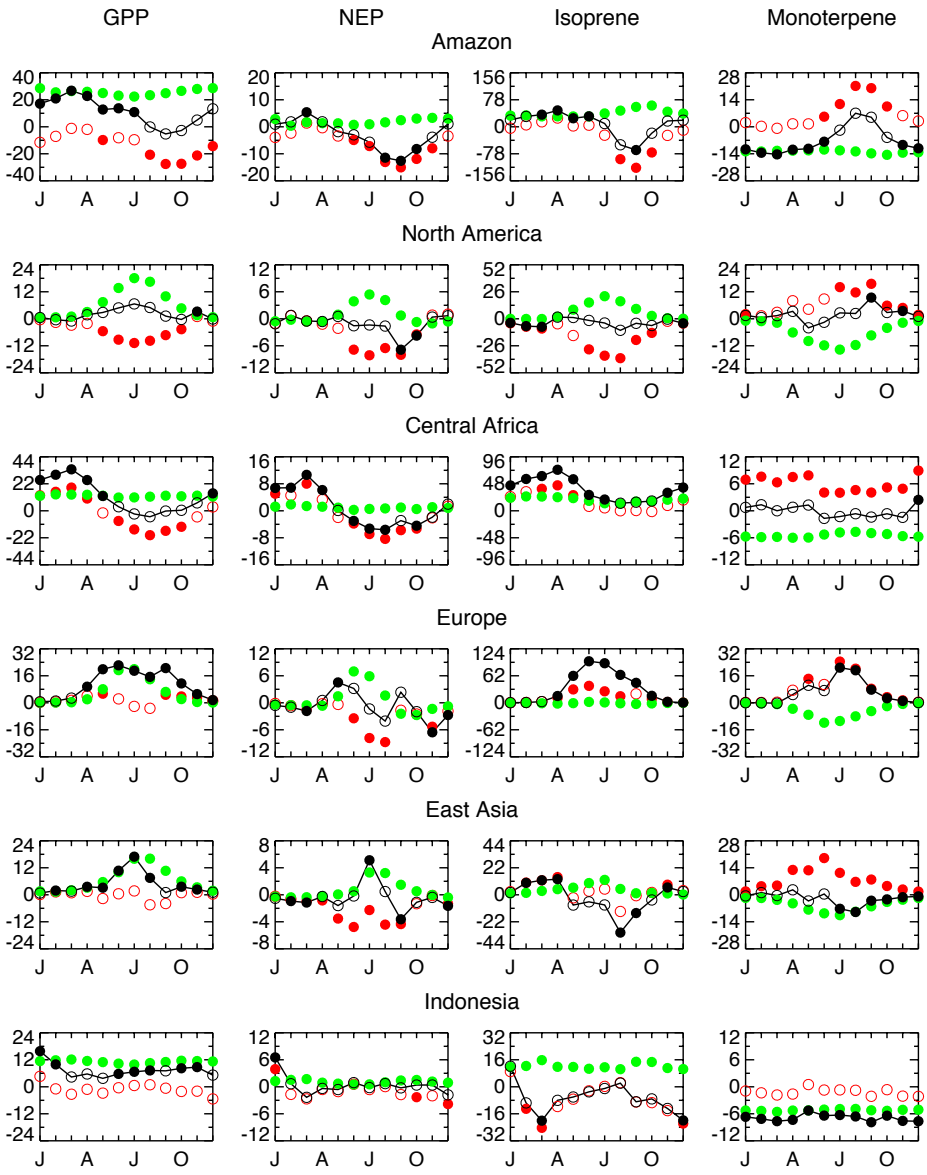


**Figure S5.** Simulated monthly trends and their drivers at six regions for 1982-2011. Different colors indicate simulations with all forcings (MET+CO2, black), meteorology alone (red), and $CO_2$ fertilization (green). Isoprene emissions are simulated with PS_BVOC scheme. Significant trends ($p < 0.05$) are denoted with filled points and vise versa.

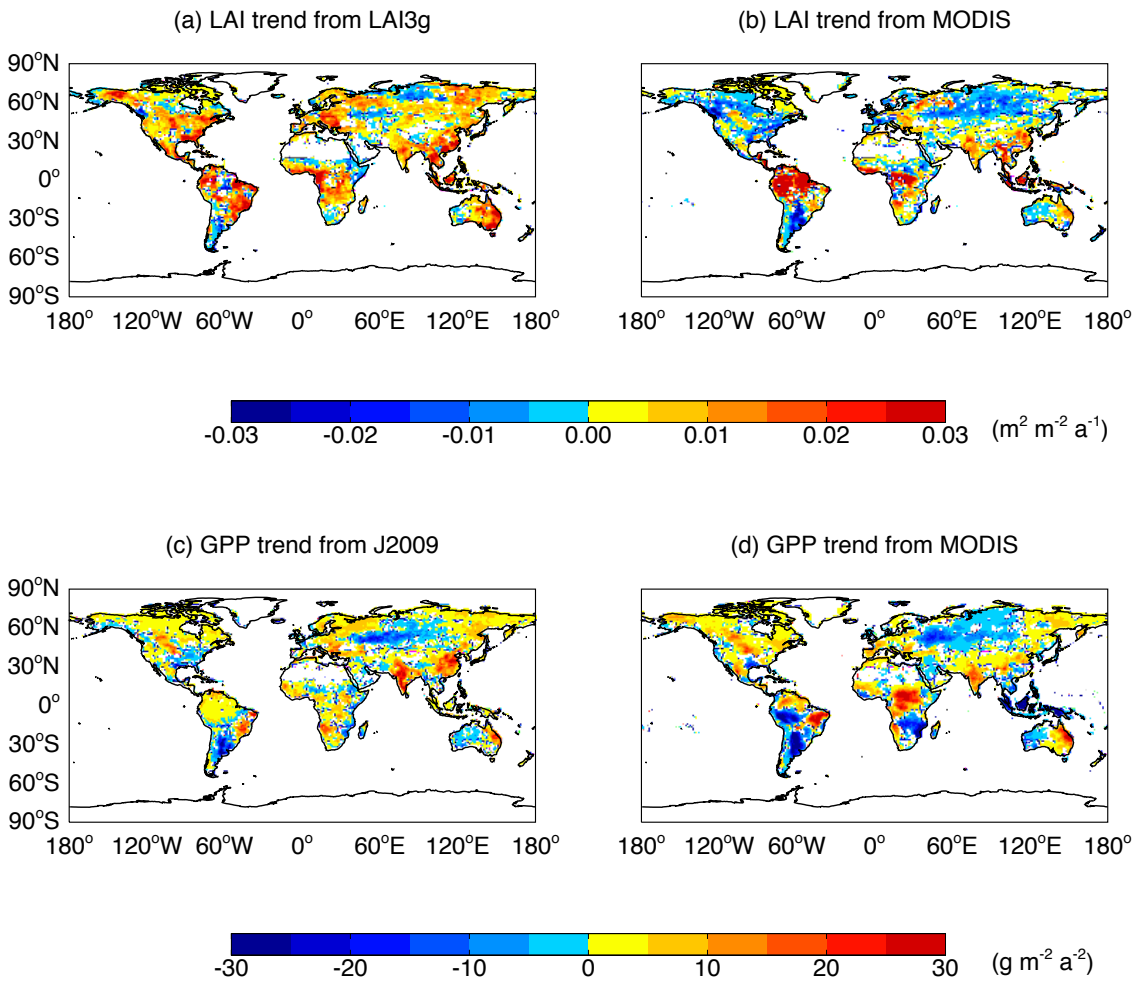


**Figure S6.** Comparison of observed trends in (a, b) leaf area index (LAI) and (c, d) GPP for 2000-2011 derived from different products. LAI measurements include data from (a) LAI3g retrieved based on the Normalized Difference Vegetation Index (NDVI) from Global Inventory Modeling and Mapping Studies (GIMMS) (Zhu et al., 2013) and (b) the Moderate Resolution Imaging Spectroradiometer (MODIS http://modis.gsfc.nasa.gov/). GPP measurements include (c) benchmark products upscaled from FLUXNET data with an ensemble of regression trees (Jung et al., 2009) and (d) remote sensing from MODIS (Zhao et al., 2005). Only the significant trends ($p < 0.1$) are presented.

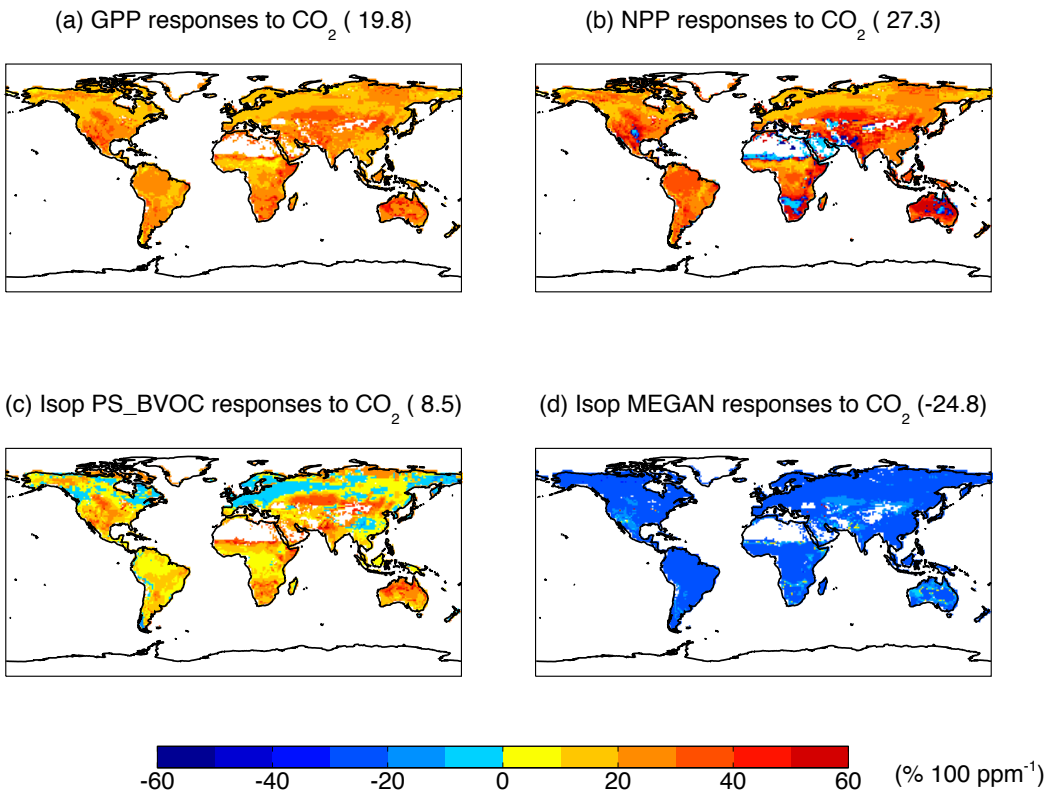


**Figure S7.** Percentage changes in (a) GPP, (b) NPP, (c) PS_BVOC isoprene, and (d) MEGAN isoprene emissions in response to elevated [$CO_2$]. At each grid square, the year-to-year total fluxes (or emissions) from simulation CO2_ONLY are linearly regressed against [$CO_2$] for 30 years. The ratios between the regression coefficients and the 30-year average fluxes (or emissions) are calculated as the responses of fluxes (or emissions) to the changes in [$CO_2$]. Only the significant ($p$<0.1) responses are presented. The global average responses are shown in the brackets.

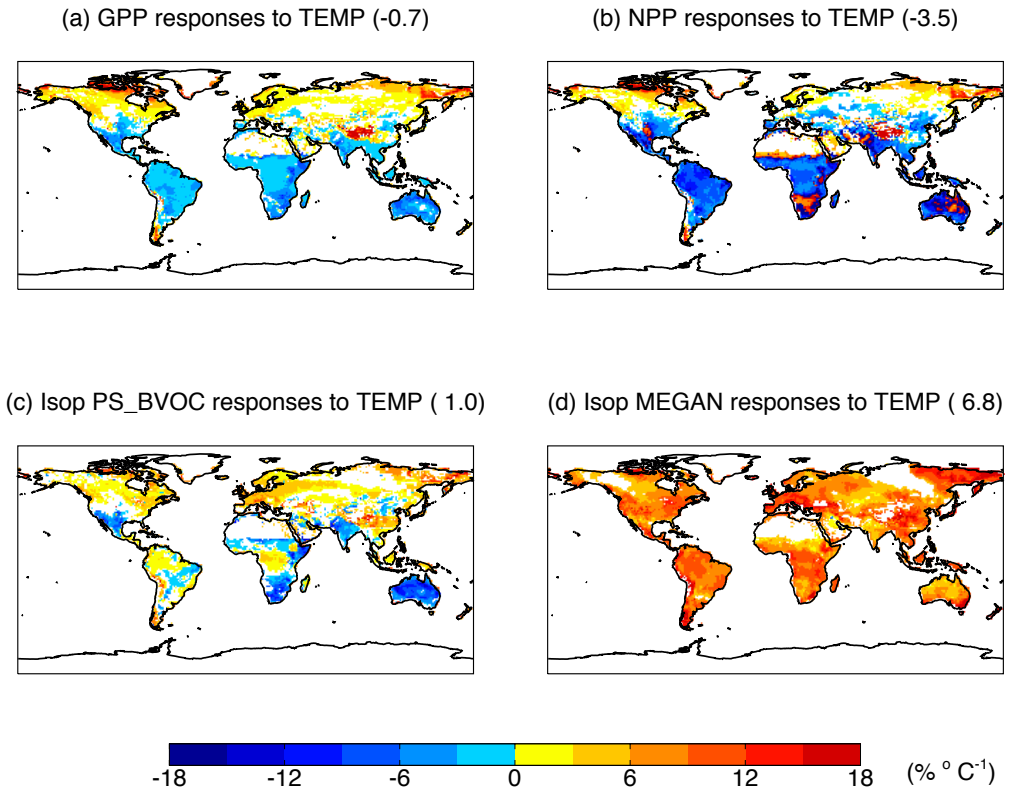


**Figure S8.** Similar to Fig. S7 but for responses to temperature based on simulation TEMP_ONLY.

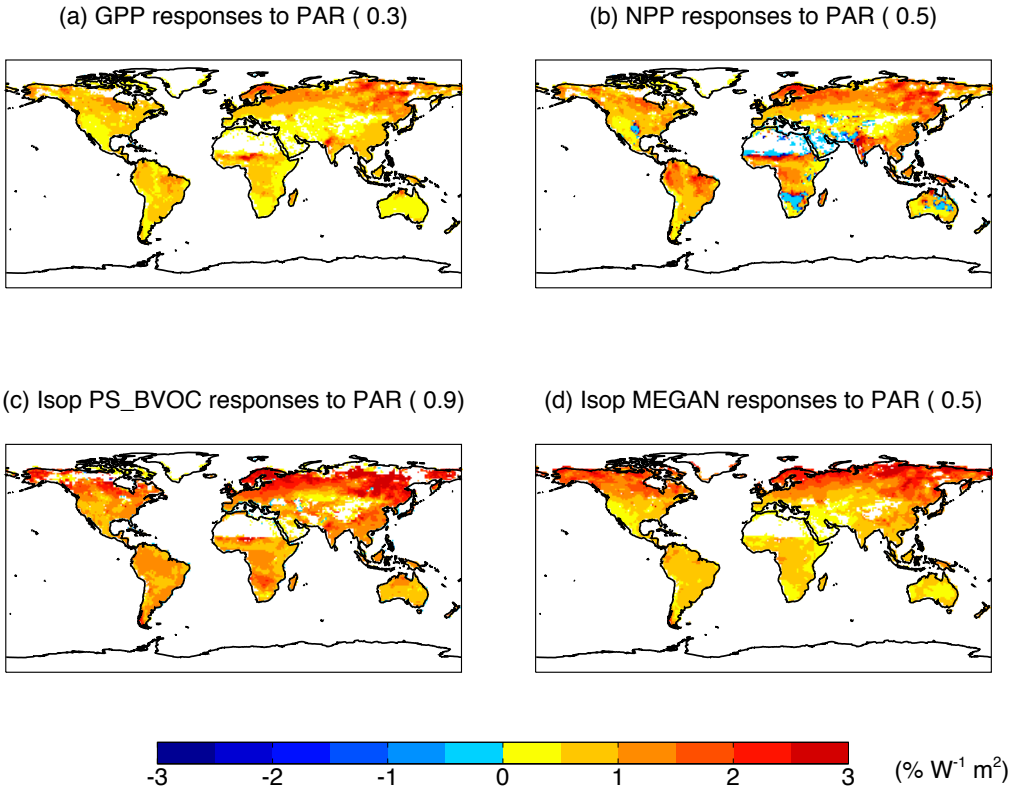


**Figure S9.** Similar to Fig. S7 but for responses to PAR based on simulation PAR_ONLY.

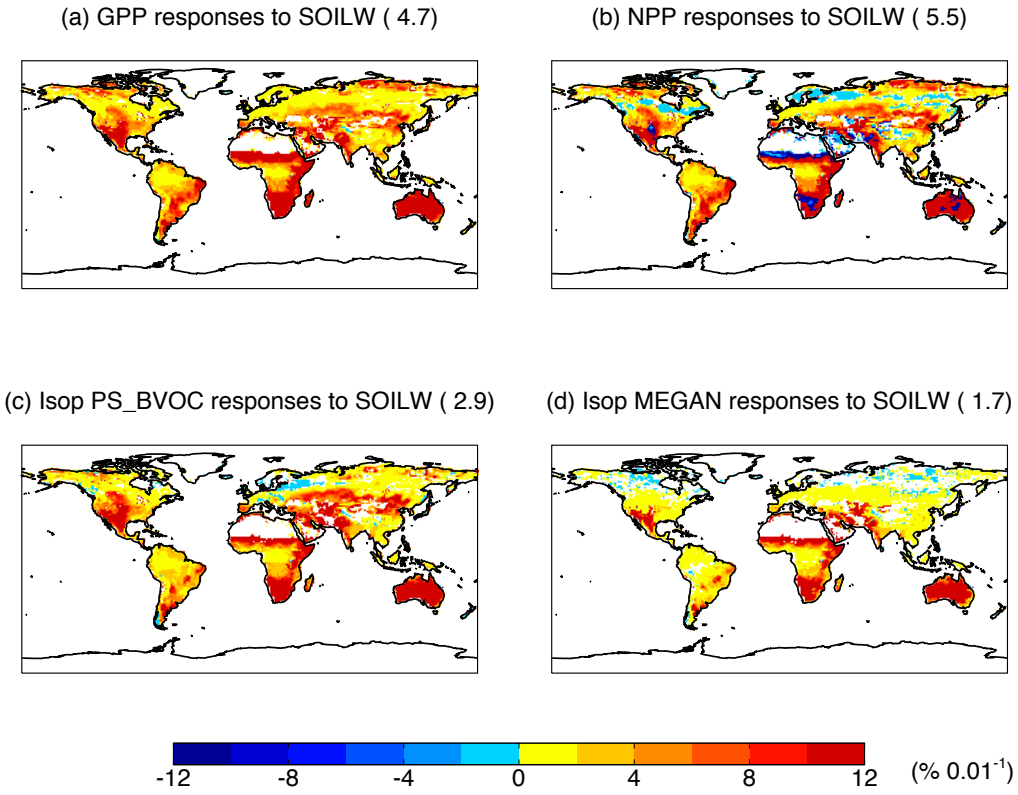


**Figure S10.** Similar to Fig. S7 but for responses to soil wetness at 1.5 m based on simulation SOILW_ONLY.

## References

Jung, M., Reichstein, M., and Bondeau, A.: Towards global empirical upscaling of FLUXNET eddy covariance observations: validation of a model tree ensemble approach using a biosphere model, Biogeosciences, 6, 2001-2013, 2009.

Zhao, M. S., Heinsch, F. A., Nemani, R. R., and Running, S. W.: Improvements of the MODIS terrestrial gross and net primary production global data set, Remote Sens Environ, 95, 164-176, doi:10.1016/J.Rse.2004.12.011, 2005.

Zhu, Z. C., Bi, J., Pan, Y. Z., Ganguly, S., Anav, A., Xu, L., Samanta, A., Piao, S. L., Nemani, R. R., and Myneni, R. B.: Global Data Sets of Vegetation Leaf Area Index (LAI)3g and Fraction of Photosynthetically Active Radiation (FPAR)3g Derived from Global Inventory Modeling and Mapping Studies (GIMMS) Normalized Difference Vegetation Index (NDVI3g) for the Period 1981 to 2011, Remote Sens-Basel, 5, 927-948, doi:10.3390/Rs5020927, 2013.